



Contents lists available at ScienceDirect

Magnetic Resonance Imaging

journal homepage: www.mrijournal.com

Improving synthesis and analysis prior blind compressed sensing with low-rank constraints for dynamic MRI reconstruction

Angshul Majumdar*

Indraprastha Institute of Information Technology Electronics and Communications Engineering, Phase III, Okhla Industrial Complex, New delhi, India

ARTICLE INFO

Article history:

Received 10 March 2014
 Revised 14 April 2014
 Accepted 25 August 2014
 Available online xxx

Keywords:

Blind compressed sensing
 Split Bregman
 Dynamic MRI reconstruction
 Matrix recovery

ABSTRACT

In blind compressed sensing (BCS), both the sparsifying dictionary and the sparse coefficients are estimated simultaneously during signal recovery. A recent study adopted the BCS framework for recovering dynamic MRI sequences from under-sampled K-space measurements; the results were promising. Previous works in dynamic MRI reconstruction showed that, recovery accuracy can be improved by incorporating low-rank penalties into the standard compressed sensing (CS) optimization framework. Our work is motivated by these studies, and we improve upon the basic BCS framework by incorporating low-rank penalties into the optimization problem. The resulting optimization problem has not been solved before; hence we derive a Split Bregman type technique to solve the same. Experiments were carried out on real dynamic contrast enhanced MRI sequences. Results show that, with our proposed improvement, the reconstruction accuracy is better than BCS and other state-of-the-art dynamic MRI recovery algorithms.

© 2014 Elsevier Inc. All rights reserved.

1. Introduction

In this work, we address the problem of reconstructing a dynamic MRI sequence from its under-sampled K-space frames. The data acquisition is expressed as follows:

$$y_t = R_t F x_t + \eta, \quad \eta \sim N(0, \sigma^2) \quad (1)$$

where x_t denotes the t^{th} frame to be reconstructed, F is the Fourier transform, R_t is the K-space sampling mask for the said instant, y_t is the acquired K-space samples and η is the noise.

Assuming that there are T such frames, (1) can be compactly represented as:

$$\text{vec}(Y) = \Phi \text{vec}(X) + \eta \quad (2)$$

where $Y = [y_1 | \dots | y_T]$, $X = [x_1 | \dots | x_T]$ and $\Phi = \text{BlockDiag}(R_t F)$.

The problem is to recover, X given Y and Φ . Usually compressed sensing (CS) [1–3] based techniques are employed to recover them. CS exploits the spatio-temporal redundancy of the sequence X in order to recover it. The spatio-temporal redundancy leads to sparsity in a transform domain, and CS techniques utilize this sparsity for recovery.

There is an alternate reconstruction approach that departs from standard CS techniques. The dynamic MRI sequence X is low-rank.

This is because the frames are temporally correlated, and hence the columns of X are not independent. Based on this argument, it was shown [4] that low-rank matrix recovery techniques can be employed to recover the dynamic MRI sequence. Unfortunately, this method cannot compete with CS based reconstruction techniques in terms of accuracy.

Some recent studies proposed combining CS based approaches with low-rank recovery techniques [5–7]. These papers showed that, such combined approaches yield better results than using sparsity based techniques or low-rank recovery techniques individually.

Recently blind compressed sensing (BCS) formulation was proposed [8]. CS assumes that the sparsifying basis is known a priori. BCS argues that, knowing the sparsifying basis is not necessary; it is possible to estimate the basis and the sparse coefficient simultaneously. Since the sparsifying basis is unknown; hence the name 'Blind'. It was shown in [9] that BCS can be used for dynamic MRI reconstruction.

The BCS technique do not explicitly incorporate the fact that the MRI sequence is low-rank; as mentioned before, exploiting this property had shown better reconstruction previously [5–7]. In this work, we propose to incorporate the low-rank property in order to improve the BCS recovery results.

The rest of the work is organized into several sections. Previous work in dynamic MRI reconstruction will be briefly discussed in the following section. Our proposed methodology is described in Section 3. The experimental results will be in Section 4. Finally, the conclusions of this work will be discussed in Section 5.

* Tel.: +919958164278.

E-mail addresses: angshul@iiitd.ac.in, angshulm@ece.ubc.ca.

2. Review of literature

The most general representation for the dynamic MRI reconstruction problem is expressed in (2). Compressed sensing (CS) based techniques exploit the spatio-temporal redundancy of the sequence for reconstruction. It is well known that MR images (columns of X) are sparse in wavelet domain. Since the sequence is temporally correlated, the variation along the rows of X can be assumed to be smooth and hence is likely to have a compact representation in the Fourier domain. In [1,2] the following formulation was proposed for recovering the sequence:

$$\min_X \|\text{vec}(Y) - \Phi \text{vec}(X)\|_2^2 + \lambda \|W \otimes F_{1D} \text{vec}(X)\|_1 \tag{3}$$

Here the W is the wavelet transform to sparsify along the spatial direction, and F_{1D} is the one dimensional Fourier transform to sparsity along the temporal direction. The Kronecker product is a convenient notation for this expression.

In [3] it was shown that one can also recover the sequence by only accounting for the temporal difference as follows:

$$\min_X \|\text{vec}(Y) - \Phi \text{vec}(X)\|_2^2 + \lambda TV_t(X) \tag{4}$$

where $TV_t = \sum \|\nabla_t X_i\|_1$ and ∇_t denotes the temporal differentiation for the i^{th} pixel.

Here the argument is that since the frames are temporally correlated, the difference between the frames is sparse, and this sparsity can be exploited for recovery.

Departing from CS based techniques, it was shown by [4] that, the matrix X can also be represented as a low-rank matrix. The argument is simple—since the frames are correlated, the columns of X are not linearly independent. In [4] a matrix factorization based technique was used for solving the recovery problem; however other techniques like nuclear norm minimization can be used as well.

More recent studies [5–7] proposed combining CS with low-rank matrix recovery. The following optimization problem is used for reconstructing X :

$$\min_X \|\text{vec}(Y) - \Phi \text{vec}(X)\|_2^2 + \lambda_1 \|\Psi_S \otimes \Psi_T \text{vec}(X)\|_1 + \lambda_2 \|X\|_* \tag{5}$$

Here Ψ_S and Ψ_T are transformed to sparsify along the spatial and temporal directions. In [5] these are respectively spatial and temporal finite differencing; in [6,7] they are wavelet and Fourier. The nuclear norm penalty ($\|X\|_*$) enforces a low-rank solution. The two parameters— λ_1 and λ_2 —balances the relative importance of the sparsity and the low-rank penalties.

So far, we have been discussing techniques where the sparsifying transform (wavelet, Fourier, finite differencing etc.) is known. A recent work [8] showed that instead of using fixed sparsifying basis, better results can be obtained if a learned basis was employed. Here dictionary learning techniques were employed to estimate the sparsifying dictionary from the training data. The learned dictionary was finally used for actual dynamic MRI reconstruction. They showed that, such a learned dictionary based reconstruction yields considerably better results than previous CS based recovery methods that used fixed sparsifying basis.

It should be noted that the prior work [8] had two phases: training—where the dictionary is estimated/learned; and testing—where the learned dictionary is employed for dynamic MRI reconstruction. The blind compressed sensing (BCS) [9] formulation marries the two phases—in BCS, both the empirical sparsifying dictionary and the sparse coefficients are estimated simultaneously during signal recovery.

In BCS, the signal is assumed to be sparse in an unknown basis, i.e. $X = DZ$ where D is the sparsifying basis and Z is the sparse coefficient

set. The BCS formulation for dynamic MRI [10] is as follows:

$$\min_{D,Z} \|\text{vec}(Y) - \Phi \text{vec}(DZ)\|_2^2 + \lambda_1 \|Z\|_1 + \lambda_2 \|D\|_F^2 \tag{6}$$

Obviously this is not a convex problem since the unknowns D and Z are in a product form (a bilinear problem). However, it has been shown in [10] that this technique yields better results than low-rank recovery techniques [4]. However, it is known that simple low-rank recovery techniques do not yield the best reconstruction results. Thus an improvement over such a technique do not mean much; one does not know if BCS can compete with state-of-the-art techniques which combine sparsity with rank deficiency, e.g. k-t SLR [5].

The BCS technique we discussed [9,10] are examples of sparse synthesis prior. A co-sparse analysis prior BCS can also be formulated [11]. The difference between synthesis and analysis prior is that the later assumes DX to be co-sparse; D being the dictionary and X being the signal of interest. The analysis prior BCS was not used for MRI reconstruction; it was used for image denoising. If this technique is adopted for dynamic MRI recovery, the optimization problem would be,

$$\min_{D,X} \|\text{vec}(Y) - \Phi \text{vec}(X)\|_2^2 + \lambda_1 \|DX\|_1 + \lambda_2 \|D\|_F^2 \tag{7}$$

In CS based MRI reconstruction, it has been observed repeatedly that the analysis prior yields better recovery results compared to the synthesis prior [12,13]. We expect that similar improvements can be achieved for BCS as well.

3. Exploiting rank-deficiency in BCS

As mentioned before, the analysis prior BCS have not been applied for dynamic MRI reconstruction. Hence it would be interesting to see how it performs. However, this may not be a significant improvement. What is even more interesting is to follow cue from prior studies [5–7] that combined rank-deficiency with sparsity based techniques. In this work, we propose to exploit the low-rank property of the MRI sequence X within the BCS reconstruction framework. This can be achieved by adding low-rank penalties to (6) and (7), leading to:

$$\min_{D,Z} \|\text{vec}(Y) - \Phi \text{vec}(DZ)\|_2^2 + \lambda_1 \|Z\|_1 + \lambda_2 \|Z\|_* + \lambda_3 \|D\|_F^2 \tag{8}$$

$$\min_{D,X} \|\text{vec}(Y) - \Phi \text{vec}(X)\|_2^2 + \lambda_1 \|DX\|_1 + \lambda_2 \|X\|_* + \lambda_3 \|D\|_F^2 \tag{9}$$

The low-rank penalty on the signal X is obvious for the co-sparse analysis prior formulation (9); since the MRI sequence is low-rank, we impose the penalty on X . For the synthesis prior (8), one might ask, why the low-rank penalty is imposed on Z . This too is simply to explain—BCS minimizes the Frobenius norm of the dictionary, hence D cannot be of low-rank; the only possibility is to impose a low-rank penalty on Z .

These formulations (8) and (9) are not convex, but then none of the BCS formulations are. Moreover, there are no algorithms to solve (8) and (9), because such problems have not been encountered before. In the following sub-section, we propose to derive efficient algorithms to solve these in the following section.

The reviewer pointed out that usually dynamic MRI sequences are acquired by multi-coil scanners. It is easy to incorporate the SENSE framework [14] into our proposed formulation. In SENSE, the data acquisition from each channel (c) is expressed as:

$$y_c = RFS_c x + \eta \tag{10}$$

where S_c is the sensitivity map for the c^{th} coil and y_c is the acquired K-space for the c^{th} coil.

Therefore, if there are C channels in all, the combined acquisition is expressed as:

$$y^{(S)} = Ex + \eta \quad (11)$$

where $y^{(S)} = \begin{bmatrix} y_1 \\ \dots \\ y_C \end{bmatrix}$ and $E = \begin{bmatrix} RFS_1 \\ \dots \\ RFS_C \end{bmatrix}$ is called the sensitivity encoding matrix.

Incorporating this into (1), we can express multi-channel dynamic MRI acquisition as:

$$y_t^{(S)} = E_t x_t + \eta \quad (12)$$

Subsequently we can modify multi-channel data acquisition for the dynamic MRI sequence as:

$$vec(Y) = \Phi vec(X) + \eta \quad (13)$$

where $Y = [y_1^{(S)} \dots y_T^{(S)}]$, $X = [x_1 \dots x_T]$ and $\Phi = BlockDiag(E_t)$.

From this formulation, one can see how BCS variants (sBCS, aBCS and our proposed techniques) can be used for recovering the dynamic MRI sequence acquired by multi-channel scanners.

3.1. Solving analysis and synthesis prior BCS problems with low-rank penalties

We solve (8) and (9) by Bregman type variable splitting with alternating directions method of multipliers (ADMM) [15]. We introduce three proxy variables— P , Q and R for the three penalty functions respectively. We add terms relaxing the equality constraints of each quantity and its proxy, and in order to enforce equality at convergence, we introduce Bregman variables B_1 , B_2 and B_3 . The new objective functions for the synthesis and the analysis prior are:

$$\min_{D,Z,P,Q,R} \|Y - \Phi vec(DZ)\|_F^2 + \lambda_1 \|P\|_1 + \lambda_2 \|Q\|_* + \lambda_3 \|R\|_F^2 + \gamma_1 \|P - Z - B_1\|_F^2 + \gamma_2 \|Q - Z - B_2\|_F^2 + \gamma_3 \|R - D - B_3\|_F^2 \quad (14)$$

$$\min_{D,X,P,Q,R} \|Y - \Phi vec(X)\|_F^2 + \lambda_1 \|P\|_1 + \lambda_2 \|Q\|_* + \lambda_3 \|R\|_F^2 + \gamma_1 \|P - DX - B_1\|_F^2 + \gamma_2 \|Q - X - B_2\|_F^2 + \gamma_3 \|R - D - B_3\|_F^2 \quad (15)$$

First, we outline the algorithm for solving the synthesis prior problem (14). The said minimization can be split into alternating minimization of the following sub-problems:

$$\min_D \|Y - \Phi vec(DZ)\|_F^2 + \gamma_3 \|R - D - B_3\|_F^2 \quad (16)$$

$$\min_Z \|Y - \Phi vec(DZ)\|_F^2 + \gamma_1 \|P - Z - B_1\|_F^2 + \gamma_2 \|Q - Z - B_2\|_F^2 \quad (17)$$

$$\min_P \lambda_1 \|P\|_1 + \gamma_1 \|P - Z - B_1\|_F^2 \quad (18)$$

$$\min_Q \lambda_2 \|Q\|_* + \gamma_2 \|Q - Z - B_2\|_F^2 \quad (19)$$

$$\min_R \lambda_3 \|R\|_F^2 + \gamma_3 \|R - D - B_3\|_F^2 \quad (20)$$

Subproblems (16), (17) and (20) are simple least squares problems that can be solved via conjugate gradient (CG). Subproblem (18) is an l_1 -norm regularized least squares problem. The standard technique to solve (18) efficiently is via iterative soft

thresholding [16]:

$$P \leftarrow Soft(Z + B_1, 2\lambda_1/\gamma_1) \quad (21)$$

where $Soft(t, u) = sign(t) \max(0, |t| - u)$.

Subproblem (19) is a least squares problem regularized by a nuclear norm penalty. This too can be efficiently solved using singular value shrinkage [17]. Here the same shrinkage operation (21) is applied on the singular values of the matrix $Z + B_2$, i.e.

$$USV^T = Z + B_2 \quad (22a)$$

$$\Sigma \leftarrow Soft(S, 2\lambda_2/\gamma_2) \quad (22b)$$

$$Q = U\Sigma V^T \quad (22c)$$

The final step is to update the Bregman relaxation variables:

$$B_1 \leftarrow P - D - B_1 \quad (23a)$$

$$B_2 \leftarrow Q - S - B_2 \quad (23b)$$

$$B_3 \leftarrow R - S - B_3 \quad (23c)$$

This concludes the algorithm for the synthesis prior problem. The analysis prior problem can be solved in a similar vein. The problem (15) can be segregated into simpler sub-problems via alternating directions:

$$\min_D \gamma_1 \|P - DX - B_1\|_F^2 + \gamma_3 \|R - D - B_3\|_F^2 \quad (24)$$

$$\min_X \|Y - \Phi vec(X)\|_F^2 + \gamma_1 \|P - DX - B_1\|_F^2 + \gamma_2 \|Q - X - B_2\|_F^2 \quad (25)$$

$$\min_P \lambda_1 \|P\|_1 + \gamma_1 \|P - DX - B_1\|_F^2 \quad (26)$$

$$\min_Q \lambda_2 \|Q\|_* + \gamma_2 \|Q - X - B_2\|_F^2 \quad (27)$$

$$\min_R \lambda_3 \|R\|_F^2 + \gamma_3 \|R - D - B_3\|_F^2 \quad (28)$$

The solution for the analysis prior sub-problems (24)–(28) remains the same as before (16)–(20). One notices that, with our proposed substitution $P = DX$, we have converted the analysis prior to an equivalent synthesis prior sub-problem (26) which can be solved as before (22).

There are two stopping criterions for the Split Bregman algorithms. Iterations continue till the objective function converges; by convergence we mean that the difference between the objective functions between two successive iterations is very small (10^{-4}). The other stopping criterion is a limit on the maximum number of iterations. We have kept it to be 500. The parameters $\gamma_1, \gamma_2, \gamma_3$ are internal to the algorithm and have been fixed at 10^{-3} ; the Bregman variables (B_1, B_2 and B_3) are all initialized to Ones'.

4. Experimental evaluation

DCE-MRI experiments were performed on female tumor bearing non-obese diabetic/severe combined immune-deficient mice. All animal experimental procedures were carried out in compliance with the guidelines of the Canadian Council for Animal Care and were approved by the institutional animal care committee. Tumor xenografts were implanted subcutaneously on the lower back region.

All images were acquired on a 7 T/30 cm bore MRI scanner (Bruker, Germany). Mice were anaesthetized with isoflurane, temperature and respiration rate were monitored throughout the experiment. FLASH was used to acquire fully sampled 2D DCE-MRI data from the implanted tumor with 42.624×19.000 mm field of view, 128×64 matrix size TR/TE = 35/2.75 ms, 40° flip angle. One thousand two hundred repetitions were performed at 2.24 s per repetition. The 2D DCE1 dataset was acquired from a mouse bearing HCT-116 tumor (human colorectal carcinoma). The animal was administered 5 $\mu\text{L/g}$ Gadovist® (Leverkusen, Germany) at 60 mM. The 2D DCE2 dataset was acquired from a mouse bearing MDA435/LCC6 tumor (human breast cancer). The animal was administered 6 $\mu\text{L/g}$ hyperbranched polyglycerol-Gd (synthesized in the Faculty of Pharmaceutical Sciences at the University of British Columbia) at 0.2 mM.

The ground-truth consists of the fully sampled K-space from which the images are reconstructed via inverse FFT. For simulating acceleration of the K-space, we used variable density random sampling. The acceleration factor was fixed at 2.5, i.e. we sampled 40% of the K-space. The reconstruction was carried out with several different reconstruction techniques

1. k-t SLR (k-t sparse and low-rank recovery) [5]
2. sBCS (synthesis prior blind compressed sensing) [10]
3. aBCS (analysis prior blind compressed sensing) [11]
4. Proposed sBCS LR (synthesis prior BCS with low-rank penalty)
5. Proposed aBCS LR (analysis prior BCS with low-rank penalty)

The implementation for k-t SLR and sBCS are available from the author's website [18]. For aBCS, we implemented the algorithm proposed by the author's of the paper. We found that this is not a very accurate or efficient algorithm—this is reflected in the results. The quantitative measure for reconstruction accuracy is normalized mean squared error (NMSE). This is shown in Table 1. The average NMSE and the standard deviation for the entire sequence are shown.

For the BCS techniques, one needs to initialize the dictionary D ; we initialized it to a DCT dictionary for the synthesis prior and a complex dualtree wavelet dictionary for the analysis prior. For aBCS and sBCS, the dictionary was initialized randomly; this was proposed in the corresponding papers [9] and [10]. The previous work on sBCS experimentally validated that the algorithm is insensitive to the size of the dictionary as long as it consists of a reasonable number of basis; they chose a dictionary size of 45. Our algorithm requires specifying the values of λ_1 , λ_2 and λ_3 ; these were experimentally determined via the L-curve method. The L-curve method can only optimally find out the value of one parameter; for more than one parameter an exhaustive search is required. In this work we used a sub-optimal strategy based on the L-curve method. First λ_2 and λ_3 were fixed to 0's, and λ_1 was found using the L-curve method. Next we find out λ_2 by the same method; here we fix λ_1 to the obtained value and λ_3 to 0. Finally we set to λ_1 and λ_2 to their obtained values and find out λ_3 by the L-curve method. This resulted in: $\lambda_1 = 10$, $\lambda_2 = .01$ and $\lambda_3 = 1$. The parameters for BCS and k-t SLR [5] were chosen based on the methodology proposed in the corresponding studies.

Generally, the analysis prior is known to yield good results, compared to the synthesis prior. But here we find that aBCS yields the worst results; even worse than the synthesis prior BCS. This is an

anomaly; most likely this is a result of the inefficient aBCS algorithm proposed in [10] to solve it.

We find that sBCS yields good results but cannot beat k-t SLR. Introducing the low-rank penalty into the BCS framework improves the results significantly—our proposed sBCS LR yields is considerably better than sBCS; it is even slightly better compared to k-t SLR. However, the best result is obtained from the analysis prior aBCS LR. The improvement from analysis prior expected and consistent from prior works [12,13].

The experiments were run on a quadcore i7 processor with 16 GB of RAM having a ZOTAC NVIDIA GeForce GTX 770 2 GB GDDR5 Graphics Card. As mentioned before the k-t SLR and the sBCS implementations were available from the author's websites. We implemented the aBCS, but using the algorithm proposed in [11]. All of them are sequential algorithms that use the CPU cores. Our proposed algorithms on the other hand are computationally more challenging—required to compute singular value decompositions in every iteration. This is the major computational bottleneck; to overcome this issue, we used a parallel algorithm for SVD that could be implemented on the GPU. Also other numerical linear operations required by our method are offloaded to the GPU. This significantly enhances the speed of our algorithms. The k-t SLR takes about 50 minutes; the sBCS takes about 300 minutes and the aBCS about the same. Our proposed sBCS LR takes about 170 minutes to run and the aBCS takes around 200 minutes. One must keep in mind that these speeds are only achievable owing to the GPU, if our algorithms are to be run on CPU's the run-times would be about an order of magnitude higher.

The quantitative results are shown in the previous table. The qualitative results are shown in terms of the reconstructed (Fig. 1) and the difference (ground-truth—reconstructed) images (Fig. 2). The difference images are contrast enhanced 5 times for visual clarity. We do not show the results from aBCS reconstruction, since the results are very poor compared to the rest. We show the results for 2 randomly chosen frames from the sequence.

It is hard to see any visible difference in reconstruction quality from the reconstructed images. For the DCE1 dataset, we have encircled regions where both k-t SLR and sBCS have introduced spurious reconstruction artifacts; for the DCE2 dataset we have encircled regions where k-t SLR and sBCS are erroneously missing certain regions that are present in the ground-truth. The improvement in reconstruction is clearly visible from the difference images (Fig. 2)—sBCS shows considerable reconstruction error; large portions of the difference image are white. The reconstruction error is slightly reduced in the sBCS. Our proposed low-rank penalty improves the result even further. The difference images are almost dark. Careful observation shows that the aBCS LR yields slightly darker (less reconstruction error) difference image compared to sBCS LR.

5. Conclusion

This work addresses the problem of recovering a dynamic MRI sequence from its sub-sampled K-space measurements. Compressed sensing (CS) based techniques exploit the sparsity of the image sequence in the transform domain for reconstruction. It has been shown that the dynamic MRI sequence can be recovered by assuming it to be a low-rank matrix. However, the best results were achieved by combining sparsity based techniques with low-rank penalties.

A recent work showed that, instead of assuming sparsity in a fixed basis, it is possible to learn the sparsifying dictionary from the data. This formulation leads to the BCS problem. It showed promising results on dynamic MRI reconstruction.

Table 1
NMSE for various techniques.

Dataset	k-t SLR (mean, std)	sBCS (mean, std)	aBCS (mean, std)	sBCS LR (mean, std)	aBCS LR (mean, std)
2 D	0.13, \pm	0.17, \pm	0.28, \pm	0.11, ± 0.04	0.10, ± 0.04
DCE1	0.051	0.110	0.189		
2 D	0.11, \pm	0.15, \pm	0.25, \pm	0.10, ± 0.04	0.09, ± 0.03
DCE2	0.047	0.112	0.180		

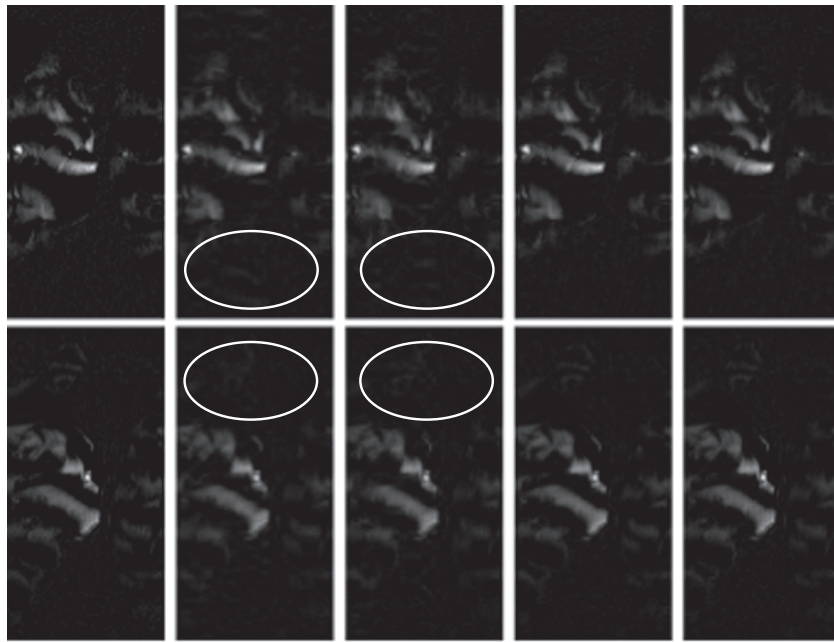


Fig. 1. Reconstructed images. Top—2D DCE1, bottom—2D DCE2. Left to right—ground-truth, k-t SLR, sBCS, sBCS LR and aBCS LR.

The original BCS formulation was constructed using the synthesis prior. It can alternatively be formulated as a co-sparse analysis prior as well. In this work, we improve the BCS formulation (both synthesis and analysis prior) by incorporating low-rank penalty. The results show better results than state-of-the-art techniques in dynamic MRI reconstruction.

However, while using BCS techniques for dynamic MRI reconstruction, one must be careful about the initialization. This is because, BCS requires solving a bi-linear non-convex optimization problem which can be stuck in a local minima. In this work, we have used DCT for initialization (sBCS too proposed DCT for initialization along with options of random initialization). The idea was that, since

MR images are known to be sparse in DCT domain, such an initialization would yield good results. Also such a fixed initialization will yield reproducible results. But DCT is not the only choice, one can also use other known sparsifying basis like wavelet or finite difference.

In this work, we have experimented with DCE MRI collected from a single coil scanner. This is because we only have access to data acquired by single coil MRI scanner. We have shown in detail, how the same techniques can be easily used with the SENSE framework for multi-coil scanners. The reviewer posed an interesting question— if the proposed formulation can be used in the calibration less multi-coil (CaLM) MRI framework [19,20]. In theory the answer is

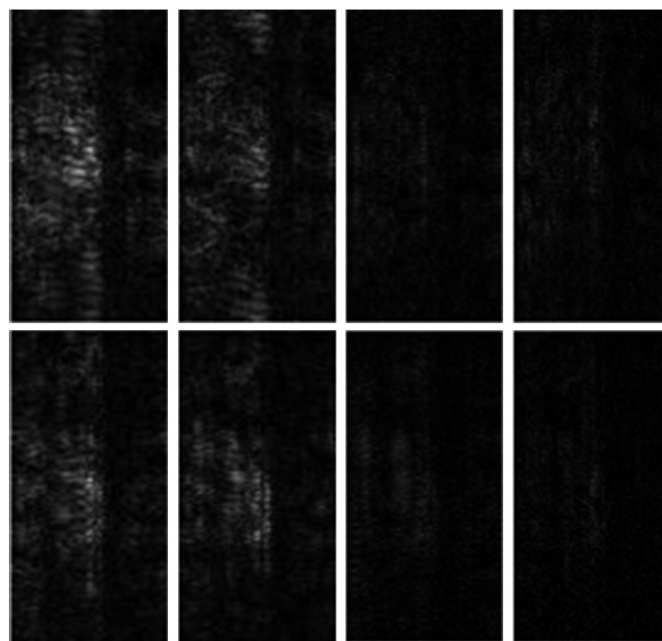


Fig. 2. Difference images. Top—2D DCE1, bottom—2D DCE2. Left to right—ground-truth, k-t SLR, sBCS, sBCS LR and aBCS LR.

affirmative, but the resulting formulation is not trivial (unlike SENSE). For each frame, the CaLM framework will formulate a row-sparse multiple measurement vector (MMV) recovery problem—coupling this with the BCS formulation is challenging. We would like to investigate this possibility in the future.

References

- [1] Gamper U, Boesiger P, Kozerke S. Compressed sensing in dynamic MRI. *Magn Reson Med* 2008;59(2):365–73.
- [2] Lustig M, Santos JM, Donoho DL, Pauly JM. “k-t SPARSE: High Frame Rate Dynamic MRI Exploiting Spatio-Temporal Sparsity” ISMRM '06; 2006.
- [3] Chen L, Schabel MC, DiBella EVR. Reconstruction of dynamic contrast enhanced magnetic resonance imaging of the breast with temporal constraints. *Magn Reson Med* 2010;28(5):637–45.
- [4] Zhao B, Haldar JP, Brinegar C, Liang ZP. Low rank matrix recovery for real-time cardiac MRI. *International Symposium on Biomedical, Imaging*; 2010. p. 996–9.
- [5] Lingala SG, Hu Y, DiBella EVR, Jacob M. Accelerated dynamic MRI exploiting sparsity and low-rank structure: k-t SLR. *IEEE Trans Med Imaging* 2011;30(5):1042–54.
- [6] Majumdar A. Improved dynamic MRI reconstruction by exploiting sparsity and rank-deficiency. *Magn Reson Imaging* 2013;31(5):789–95.
- [7] Majumdar A, Ward RK, Aboulnasr T. “Non-Convex Algorithm for Sparse and Low-Rank Recovery: Application to Dynamic MRI Reconstruction”. *Magn Reson Imaging* 2012;Vol. 31(3):448–55.
- [8] Caballero J, Price AN, Rueckert D, Hajnal JV. Dictionary learning and time sparsity for dynamic MR data reconstruction. *IEEE Trans Med Imaging* 2014;33(4):979–94.
- [9] Gleichman S, Eldar YC. Blind compressed sensing. *IEEE Trans Inf Theory* 2011;57:6958–75.
- [10] Lingala SG, Jacob M. Blind compressed sensing dynamic MRI. *IEEE Trans Med Imaging* 2013;32:1132–45.
- [11] Wörmann J, Hawe S, Kleinsteuber M. Analysis based blind compressive sensing. *IEEE Signal Process Lett* 2013;20(5):491–4.
- [12] Majumdar A, Ward RK. Under-determined non-Cartesian MR reconstruction. *MICCAI 2010*:513–20.
- [13] Majumdar A, Ward RK. On the choice of compressed sensing priors: an experimental study. *Signal Process Image Commun* 2012;27(9):1035–48.
- [14] Pruessmann KP, Weiger M, Scheidegger MB, Boesiger P. SENSE: sensitivity encoding for fast MRI. *Magnetic Resonance in Medicine* 1999;42:952–62.
- [15] Wohlberg B, Chartrand R, Theiler J. Local principal component pursuit for nonlinear datasets. *IEEE International Conference on Acoustics, Speech, and Signal Processing*; 2012. p. 3925–8.
- [16] Daubechies I, Defrise M, De Mol C. An iterative thresholding algorithm for linear inverse problems with a sparsity constraint. *Communications on Pure and Applied Mathematics*, 57; 2004 1413–57.
- [17] Majumdar A, Ward RK. Some empirical advances in matrix completion. *Signal Process* 2011;91:1334–8.
- [18] <http://research.engineering.uiowa.edu/cbig/content/software>.
- [19] Majumdar Angshul, Ward Rabab K. Calibration-less multi-coil MR image reconstruction. *Magn Reson Imaging* 2012;30(7):1032–45.
- [20] Chen Chen, Li Yeqing, Huang Junzhou. Calibrationless parallel MRI with joint total variation regularization. *Medical Image Computing and Computer-Assisted Intervention-MICCAI 2013*. Berlin Heidelberg: Springer; 2013. p. 106–14.